Report: Advanced Model Based Design and Testing of Marine Control Systems

Jens Alfsen
Magnus Feldt Paulsen
Martin Kvisvik Larsen

November 2019

1 Introduction

This report documents the work conducted on a project in the module-course TMR4515 at NTNU during the fall of 2019. The project revolves around handling stochastic processes through the use of Kalman filters and dynamic hypothesis testing (DHT). The project consists of two tasks. The first task is to implement a discrete Kalman filter, for a process corrupted by process and measurement noise. The second task is to implement DHT for three basis hypotheses, in order to account for uncertain and varying physical parameters. The physical system consists of two motors and two loads, connected through flexible transmission.

2 Models

2.1 Continuous-time Model

By applying Newton's second law of motion and given that the process- and measurement noises are Gaussian white noises, a continuous-time state-space representation of the plant noise can be found as

$$\dot{\mathbf{x}} = \mathbf{A}\mathbf{x}(t) + \mathbf{B}\mathbf{u}(t) + \mathbf{G}\mathbf{w}(t), \quad \mathbf{w} \sim \mathcal{N}(\mathbf{0}, \mathbf{Q}_n\delta(t-\tau)), \quad \mathbf{Q}_n = \begin{bmatrix} \sigma_{w_1}^2 & 0 \\ 0 & \sigma_{w_2}^2 \end{bmatrix} \tag{1a}$$

$$\mathbf{y}(t) = \mathbf{C}\mathbf{x}(t) + \mathbf{v}(t), \quad \mathbf{v} \sim \mathcal{N}(\mathbf{0}, \mathbf{R}_n\delta(t-\tau)), \quad \mathbf{R}_n = \begin{bmatrix} \sigma_{\theta_{L1}}^2 & 0 \\ 0 & \sigma_{\theta_{L2}}^2 \end{bmatrix} \tag{1b}$$

where the state vector is $\mathbf{x}(t) = \begin{bmatrix} \theta_{L1} & \theta_{M1} & \theta_{M2} & \theta_{L2} & \omega_{L1} & \omega_{M1} & \omega_{M2} & \omega_{L2} & d_1 & d_2 \end{bmatrix}^\top$ and the measurements $\mathbf{y} = \begin{bmatrix} \theta_{L1} & \theta_{L2} \end{bmatrix}^\top$. The system matrices $\mathbf{A}$, $\mathbf{B}$, $\mathbf{G}$ and $\mathbf{C}$ can in found in appendix 1.1. The value of all the parameters are known, except for k_2 and k_5 which are unknown but assumed to have values in the intervals $k_2 \in [0.75, 2.5]$ and $k_5 \in [0.9, 2.5]$. The intensities of the process noises, $\sigma_{w_1}^2$ and $\sigma_{w_2}^2$, are given as unity, while the intensities of the measurement noises, $\sigma_{\theta_{L1}}^2$ and $\sigma_{\theta_{L2}}^2$, are given as 10^{-6}. Due to the stochastic noises in eq. (1), the system is no longer deterministic, but rather a stochastic dynamic system.

2.2 Discretization

The system in eq. (1) is a continuous linear time-invariant (LTI) system. Due to the nature of digital devices, for practical implementations a discretization of the continuous LTI sytem must be performed. From basic control theory, under the assumption that the control input is produced by a zero-order hold and that the process noise and measurement noise are Guassian, the solution to eq. (1) can be written as (Brekke (2019))

$$\mathbf{x}_k = \mathbf{A}_d\mathbf{x}_{k-1} + \mathbf{B}_d\mathbf{u}_k + \mathbf{w}_k, \quad \mathbf{w}_k \sim \mathcal{N}(\mathbf{0}, \mathbf{Q}_d) \tag{2a}$$

$$\mathbf{y}_k = \mathbf{C}\mathbf{x}_k + \mathbf{v}_k, \quad \mathbf{v}_k \sim \mathcal{N}(\mathbf{0}, \mathbf{R}_d) \tag{2b}$$

where the matrices $\mathbf{A}_d$ and $\mathbf{B}_d$ and vector $\mathbf{w}_k$ are given by:

$$\mathbf{A}_d = e^{\mathbf{A}(t_k - t_{k-1})}, \quad \mathbf{B}_d = \int_{t_{k-1}}^{t_k} e^{\mathbf{A}(t_k-\tau)}\mathbf{B}d\tau, \quad \mathbf{w}_k = \int_{t_{k-1}}^{t_k} e^{\mathbf{A}(t_k-\tau)}\mathbf{G}\mathbf{w}(\tau)d\tau \tag{3a}$$

Given that the sampling time interval $T = t_k - t_{k-1}$ is constant, the discrete time transition matrix $\mathbf{A}_d$ and input matrix $\mathbf{B}_d$ can be found using Van Loan's formula as

$$\exp\left(\begin{bmatrix} \mathbf{A} & \mathbf{B} \\ \mathbf{0} & \mathbf{0} \end{bmatrix} T \right) = \begin{bmatrix} \mathbf{N}_{11} & \mathbf{N}_{12} \\ \mathbf{N}_{21} & \mathbf{N}_{22} \end{bmatrix} \tag{4a}$$

$$\mathbf{A}_d = \mathbf{N}_{11} \tag{4b}$$

$$\mathbf{B}_d = \mathbf{N}_{12} \tag{4c}$$

The instantaneous covariance matrix of the discrete time process noise $\mathbf{Q}_d$ is given as:

$$\mathbf{Q}_d = E[\mathbf{w}_k \mathbf{w}_k^\top] = \int_0^T e^{\mathbf{A}(T-\tau)} \mathbf{G} \mathbf{Q}_n \mathbf{G}^\top e^{\mathbf{A}^\top (T-\tau)} d\tau \tag{5}$$

A closed-form solution for $\mathbf{Q}_d$ in eq. (5) can be obtained from Van Loan's formula, similarly to $\mathbf{A}_d$ and $\mathbf{B}_d$:

$$\exp\left(\begin{bmatrix} -\mathbf{A} & \mathbf{G}\mathbf{A}\mathbf{G}^\top \\ \mathbf{0} & \mathbf{A}^\top \end{bmatrix} T \right) = \begin{bmatrix} \mathbf{M}_{11} & \mathbf{M}_{12} \\ \mathbf{M}_{21} & \mathbf{M}_{22} \end{bmatrix} \tag{6a}$$

$$\mathbf{Q}_d = \mathbf{M}_{22}^\top \mathbf{M}_{12} \tag{6b}$$

The instantaneous measurement noise covariance matrix is given as the intensity of the continous time measurement white noise averaged over the sampling period, i.e.:

$$\mathbf{R}_d = \frac{1}{T} \mathbf{R}_n = \frac{1}{T} \begin{bmatrix} \sigma_{\theta_{L1}}^2 & 0 \\ 0 & \sigma_{\theta_{L2}}^2 \end{bmatrix} \tag{7}$$

3 Exercise One: Kalman Filter Design

3.1 Exercise Description

In order to perform filtering a discrete time Kalman Filter is to be designed under the assumption that the values for k_2 and k_5 are known. In order to validate the Kalman Filter implementation filter consistency is checked by analyzing the sequence of normalized innovations squared (NIS). Necessary background theory is also presented.

3.2 Theory

In the filtering problem, the goal is to estimate the state of a stochastic dynamic system from a series of noisy measurements and, possibly, the control inputs. The problem can be formulated in a probabilistic setting by two models, i.e. the process model $p(\mathbf{x}_k|\mathbf{x}_{k-1}, \mathbf{u}_k)$ and the measurement model $p(\mathbf{y}_k|\mathbf{x}_k)$ (Brekke (2019)). Here, the Markov property has implicitly been assumed for the probabilistic models, meaning that the probability distribution of $\mathbf{x}_k$ and $\mathbf{y}_k$ do not depend on the entire time series of previous $\mathbf{x}_i$ and $\mathbf{u}_i$, but only on the previous state $\mathbf{x}_{k-1}$ and the current control input $\mathbf{u}_k$ and the current state $\mathbf{x}_k$, respectively. In this setting an optimal filter is the Bayes filter, which can be derived from the theorem of total probability and Bayes' rule as

$$p(\mathbf{x}_k|\mathbf{y}_{1:k-1}, \mathbf{u}_{1:k}) = \int p(\mathbf{x}_k, \mathbf{x}_{k-1}|\mathbf{y}_{1:k-1}, \mathbf{u}_{1:k}) d\mathbf{x}_{k-1} = \int p(\mathbf{x}_k|\mathbf{x}_{k-1}, \mathbf{u}_k) p(\mathbf{x}_{k-1}|\mathbf{y}_{1:k-1}, \mathbf{u}_{1:k-1}) d\mathbf{x}_{k-1} \tag{8a}$$

$$p(\mathbf{x}_k|\mathbf{y}_{1:k}, \mathbf{u}_{1:k}) = \frac{p(\mathbf{y}_k|\mathbf{x}_k) p(\mathbf{x}_k|\mathbf{y}_{1:k-1}, \mathbf{u}_{1:k})}{p(\mathbf{y}_k|\mathbf{y}_{1:k-1}, \mathbf{u}_{1:k})} \propto p(\mathbf{y}_k|\mathbf{x}_k) p(\mathbf{x}_k|\mathbf{y}_{1:k-1}, \mathbf{u}_{1:k}) \tag{8b}$$

where eq. (8a) and eq. (8b) are known as the prediction- and update step, respectively. In eq. (8a) one can see that current prediction step is dependent on the process model $p(\mathbf{x}_k|\mathbf{x}_{k-1}, \mathbf{u}_k)$ and the previous update step $p(\mathbf{x}_{k-1}|\mathbf{y}_{1:k-1}, \mathbf{u}_{1:k-1})$. The current update step is on the other hand dependent on the measurement model $p(\mathbf{y}_k|\mathbf{x}_k)$ and the current prediction step $p(\mathbf{x}_k|\mathbf{y}_{1:k-1}, \mathbf{u}_{1:k})$. From eq. (2) it is evident that for a given previous state $\mathbf{x}_{k-1}$, control input $\mathbf{u}_k$ and current state $\mathbf{x}_k$, the probability distributions of $\mathbf{x}_k$ and $\mathbf{y}_k$ inherent their gaussianity and whiteness from the process- and measurement noise, respectively. Due to the recursive nature of the Bayes filter an initial distribution, also known as a prior, has to be assigned. Just like the process- and measurement model, the prior is assumed to be Gaussian. The distributions of the process model, measurement model and prior can then be written, respectively, as

$$p(\mathbf{x}_k|\mathbf{x}_{k-1}, \mathbf{u}_k) = \mathcal{N}(\mathbf{x}_k; \mathbf{A}_d \mathbf{x}_{k-1} + \mathbf{B}_d \mathbf{u}_k, \mathbf{Q}_d) \tag{9a}$$

$$p(\mathbf{y}_k|\mathbf{x}_k) = \mathcal{N}(\mathbf{y}_k; \mathbf{C}\mathbf{x}_k, \mathbf{R}_d) \tag{9b}$$

$$p(\mathbf{x}_0) = \mathcal{N}(\mathbf{x}_0; \hat{\mathbf{x}}_0, \hat{\mathbf{P}}_0) \tag{9c}$$

Under these conditions close-form expressions for eq. (8a) and eq. (8b) can be found. Using the product identity, a fundamental property of Gaussians, the prediction and update step of the Bayes filter become (Brekke (2019))

$$\begin{aligned} p(\mathbf{x}_k|\mathbf{y}_{1:k-1}, \mathbf{u}_{1:k}) &= \int \mathcal{N}(\mathbf{x}_k; \mathbf{A}_d\mathbf{x}_{k-1} + \mathbf{B}_d\mathbf{u}_k, \mathbf{Q}_d) \cdot \mathcal{N}(\mathbf{x}_{k-1}; \bar{\mathbf{x}}_{k-1}, \bar{\mathbf{P}}_{k-1}) d\mathbf{x}_{k-1} \\ &= \mathcal{N}(\mathbf{x}_k; \mathbf{A}_d\bar{\mathbf{x}}_{k-1} + \mathbf{B}_d\mathbf{u}_k, \mathbf{A}_d\bar{\mathbf{P}}_{\mathbf{k-1}}\mathbf{A}_d^\top + \mathbf{Q}_d) \cdot \int \mathcal{N}(\mathbf{x}_{k-1}; \boldsymbol{\mu}_{k-1}, \boldsymbol{\Sigma}_{k-1}) d\mathbf{x}_{k-1} \\ &= \mathcal{N}(\mathbf{x}_k; \mathbf{A}_d\bar{\mathbf{x}}_{k-1} + \mathbf{B}_d\mathbf{u}_k, \mathbf{A}_d\bar{\mathbf{P}}_{\mathbf{k-1}}\mathbf{A}_d^\top + \mathbf{Q}_d) \cdot 1 \\ &= \mathcal{N}(\mathbf{x}_k; \hat{\mathbf{x}}_k, \hat{\mathbf{P}}_k) \end{aligned} \tag{10a}$$

$$\begin{aligned} p(\mathbf{x}_k|\mathbf{y}_{1:k}, \mathbf{u}_{1:k}) &= \mathcal{N}(\mathbf{y}_k; \mathbf{C}\mathbf{x}_k, \mathbf{R}_d) \cdot \mathcal{N}(\mathbf{x}_k; \hat{\mathbf{x}}_k, \hat{\mathbf{P}}_k) \\ &= \mathcal{N}(\mathbf{y}_k; \mathbf{C}\hat{\mathbf{x}}_k, \mathbf{C}\hat{\mathbf{P}}_k\mathbf{C}^\top + \mathbf{R}_d) \cdot \mathcal{N}(\mathbf{x}_k; \hat{\mathbf{x}}_k + \mathbf{L}_k(\mathbf{y}_k - \mathbf{C}\hat{\mathbf{x}}_k), (\mathbf{I} - \mathbf{L}_k\mathbf{C})\hat{\mathbf{P}}_k) \\ &= \mathcal{N}(\mathbf{y}_k; \hat{\mathbf{y}}_k, \mathbf{S}_k) \cdot \mathcal{N}(\mathbf{x}_k; \bar{\mathbf{x}}_k, \bar{\mathbf{P}}_k) \\ &\propto \mathcal{N}(\mathbf{x}_k; \bar{\mathbf{x}}_k, \bar{\mathbf{P}}_k) \end{aligned} \tag{10b}$$

where the expression for $\mathbf{L}_k$, commonly known as the Kalman gain, is

$$\mathbf{L}_k = \hat{\mathbf{P}}_k\mathbf{C}^\top\mathbf{S}_k^{-1} \tag{11}$$

One can see that the Kalman filter is realization of the Bayes filter in the case of a linear process- and measurement model and Gaussian noises. Iteratively calculating the means and covariances of eq. (10a) and eq. (10b), using the more numerically stable Joseph form for $\bar{\mathbf{P}}_k$, leads to the Kalman filter in algorithm 1.

Algorithm 1: The Kalman Filter

Data: $\bar{\mathbf{x}}_{k-1}$, $\bar{\mathbf{P}}_{k-1}$, $\mathbf{y}_k$, $\mathbf{u}_k$
Result: $\bar{\mathbf{x}}_k$, $\bar{\mathbf{P}}_k$
$\hat{\mathbf{x}}_k = \mathbf{A}_d\bar{\mathbf{x}}_{k-1} + \mathbf{B}_d\mathbf{u}_k$
$\hat{\mathbf{P}}_k = \mathbf{A}_d\bar{\mathbf{P}}_{k-1}\mathbf{A}_d^\top + \mathbf{Q}_d$
$\hat{\mathbf{y}}_k = \mathbf{C}\hat{\mathbf{x}}_k$
$\boldsymbol{\nu}_k = \mathbf{y}_k - \hat{\mathbf{y}}_k$
$\mathbf{S}_k = \mathbf{C}\hat{\mathbf{P}}_k\mathbf{C}^\top + \mathbf{R}_d$
$\mathbf{L}_k = \hat{\mathbf{P}}_k\mathbf{C}^\top\mathbf{S}_k^{-1}$
$\bar{\mathbf{x}}_k = \hat{\mathbf{x}}_k + \mathbf{L}_k\boldsymbol{\nu}_k$
$\bar{\mathbf{P}}_k = (\mathbf{I} - \mathbf{L}_k\mathbf{C})\hat{\mathbf{P}}_k(\mathbf{I} - \mathbf{L}_k\mathbf{C})^\top + \mathbf{L}_k\mathbf{R}_d\mathbf{L}_k^\top$

The quantity $\boldsymbol{\nu}_k$, also known as innovation, has the distribution $\mathcal{N}(\boldsymbol{\nu}_k; \mathbf{0}, \mathbf{S}_k)$. It can be shown that the normalized innovation squared (NIS) is distributed as

$$\text{NIS}_k = \boldsymbol{\nu}_k^\top\mathbf{S}_k^{-1}\boldsymbol{\nu}_k \sim \chi^2(d) \tag{12}$$

where the degrees of freedom, d, is the number of innovations, which in this case is the same as the number of measurements. The sequence of NISes can be used to check filter consistency. This is done by setting up a $1 - \alpha$ confidence interval and checking the fraction of NISes that fall within it is close to $1 - \alpha$.

3.3 Results

Parameter	Value	Parameter Description
$k_{2,\text{Plant}}$	1.625	Plant model parameter
$k_{5,\text{Plant}}$	1.7	Plant model parameter
$k_{2,\text{KF}}$	1.625	Kalman filter model parameter
$k_{5,\text{KF}}$	1.7	Kalman filter model parameter
$\hat{\mathbf{x}}_0$	$[0,0,0,0,0,0,0,0,0,0]^\top$	Prior state estimates
$\hat{\mathbf{P}}_0$	$\text{diag}\left(0.1^2, 0.1^2, 0.1^2, 0.1^2, 0.1^2, 0.1^2, 0.1^2, 0.1^2, 0.1^2, 0.1^2\right)$	Prior covariance estimates

Table 1: Parameters for the plant model and the Kalman filter model for task 1.

Metric	Value	Unit	Metric Description
MSE	0.00197	rad^2	Measurement mean squared error
RMSE	0.04439	rad	Measurement root mean squared error
$\overline{\text{NIS}}$	0.95	–	Fraction of NISes with 95% CI

Table 2: Performance metrics for the Kalman filter for task 1.

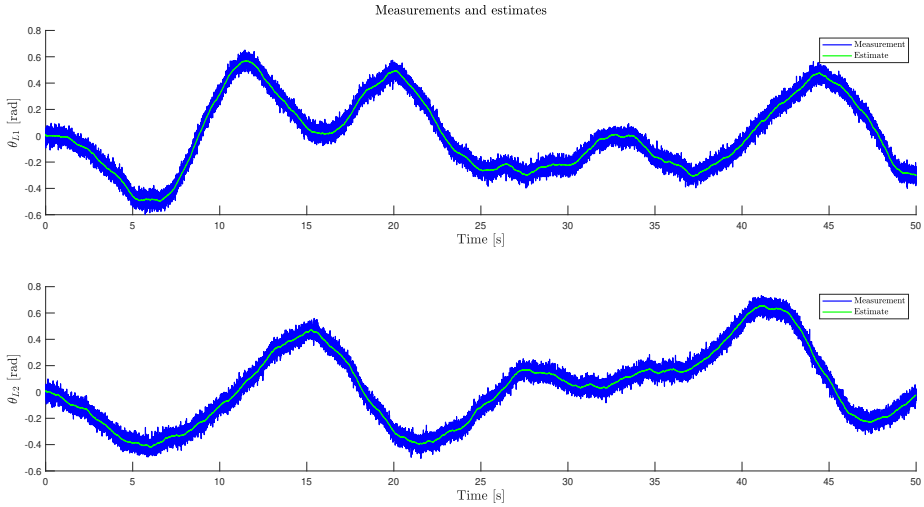

Figure 1: Noisy measurements and Kalman filter measurement estimates.

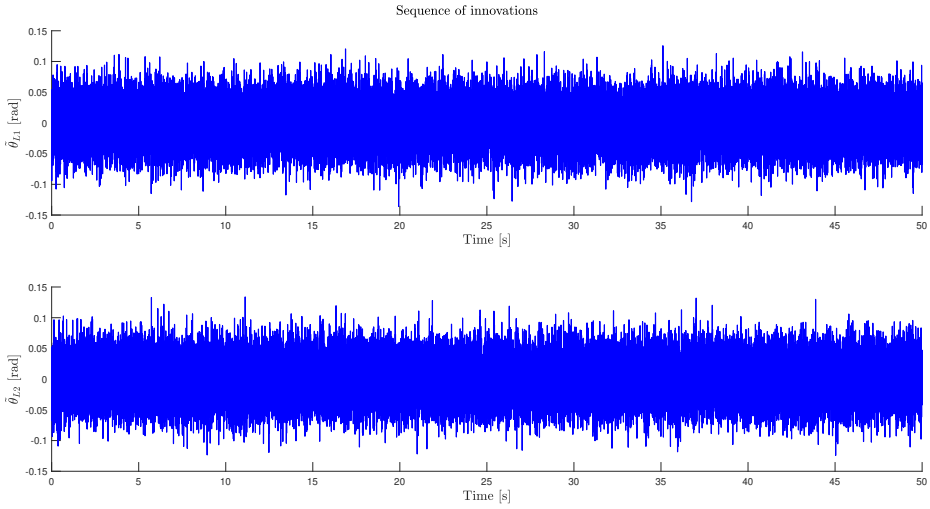

Figure 2: Sequence of innovations.

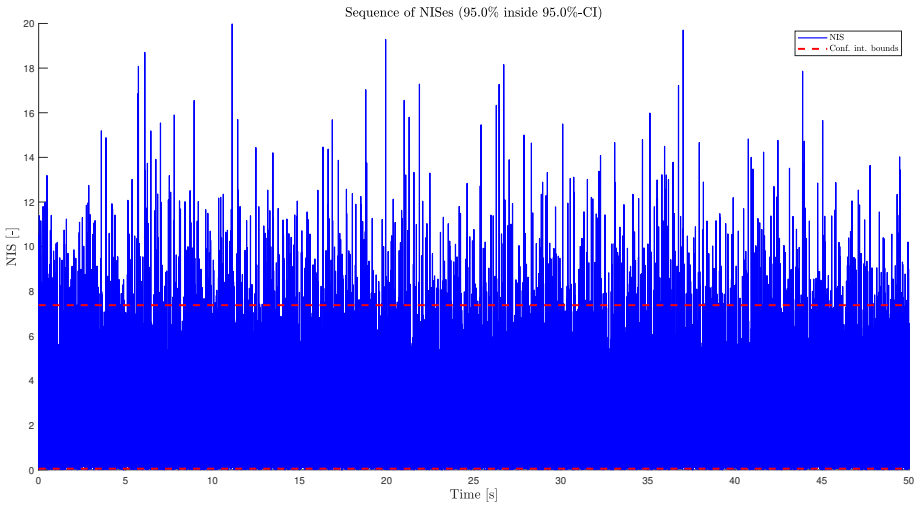

Figure 3: Sequence of NISes and corresponding 95% confidence interval bounds.

3.4 Discussion

Figure 1 shows the filtering effect of the Kalman filter, illustrated through the green line representing $\bar{\theta}_{L1}$ and $\bar{\theta}_{L2}$. For feedback control systems this is essential, in order to obtain precise control action and avoiding oscillation of the actuators. Figure 2 shows the filter innovations. The resulting innovations resemble white-noise, suggesting that the filter was correctly implemented. In fig. 3 one can see the sequence of NISes and their 95% confidence interval bounds. For real life applications where the plant model, process noise and measurement noise are unknown, analyzing filter consistency through the sequence of NISes is an important aspect of tuning a Kalman filter. For simulations, where the plant model is known, the sequence of NISes can be used to verify the Kalman filter implementation and correct discretization of the process model. In our case one can see that 95% of the NISes fall within their 95% confidence interval, suggesting that the Kalman filter implementation and process model discretization are correct. Additionally, from table 2 one can see that mean squared error (MSE) and root mean squared error (RMSE) between the measured angles, θ_{L1} and θ_{L2} and the predicted angles, $\hat{\theta}_{L1}$ and $\hat{\theta}_{L2}$, are in the order of 10^{-3} and 10^{-2} respectively.

4 Exercise two: Designing Dynamic Hypothetic Testing

4.1 Exercise Description

The parameters k_2 and k_5 are unknown in this task. The parameter space of the unknown parameters is divided into three subspaces:

- $\Omega_1 = \{k_2 \in [1.25, 2.5], k_5 \in [1.5, 2.5]\}$
- $\Omega_2 = \{k_2 \in [0.75, 1.25], k_5 \in [0.75, 2.5]\}$
- $\Omega_3 = \{k_2 \in [1.25, 2.5], k_5 \in [0.75, 1.5]\}$

In order to do inference on the unknown parameters three hypotheses are formulated, one in each of the three parameter subspaces, as

- $\mathcal{H}_1$: $k_2 = 2$, $k_5 = 2$.
- $\mathcal{H}_2$: $k_2 = 1$, $k_5 = 1.75$.
- $\mathcal{H}_3$: $k_2 = 2$, $k_5 = 1.25$.

For each of the three hypotheses a Kalman filter and a steady-state Kalman filter is implemented. The three Kalman filters and the three steady-state Kalman filters are then assembled in two different ensemblies in order to perform dynamic hypothesis testing (DHT).

4.2 Theory

For a linear plant it can be shown that the covariance estimate $\bar{\mathbf{P}}_k$, and consequently $\mathbf{L}_k$, will converge to a steady-state configuration. This is not evident from the probabilistic derivation in eq. (10b), but can be shown through the derivation of the Kalman filter from a signal processing perspective (Brown and Hwang (2012)). By utilizing the steady-state solution the Kalman filter gain $\mathbf{L}_\infty$ and covariance matrix $\bar{\mathbf{P}}_\infty$ can be calculated offline as opposite to algorithm 1, which has to be calculated online in an recursive manner.

In order to perform dynamic hypothesis testing the likelihood of different probabilities must be derived. The likelihood of the hypothesis $\mathcal{H}_i$ is the probability of hypothesis $\mathcal{H}_i$ given the series of measurements and control inputs, expressed as $\Pr(\mathcal{H}_i|\mathbf{y}_{1:k}, \mathbf{u}_{1:k})$. By applying Bayes' rule and the theorem of total probability the expression can further be written as

$$\begin{aligned}\Pr(\mathcal{H}_i|\mathbf{y}_{1:k}, \mathbf{u}_{1:k}) &= \frac{p(\mathbf{y}_k|\mathcal{H}_i, \mathbf{y}_{1:k-1}, \mathbf{u}_{1:k})\Pr(\mathcal{H}_i|\mathbf{y}_{1:k-1}, \mathbf{u}_{1:k-1})}{p(\mathbf{y}_k|\mathbf{y}_{1:k-1}, \mathbf{u}_{1:k})} \\ &= \frac{p(\mathbf{y}_k|\mathcal{H}_i, \mathbf{y}_{1:k-1}, \mathbf{u}_{1:k})\Pr(\mathcal{H}_i|\mathbf{y}_{1:k-1}, \mathbf{u}_{1:k-1})}{\sum_{j=1}^{3} p(\mathbf{y}_k|\mathcal{H}_j, \mathbf{y}_{1:k-1}, \mathbf{u}_{1:k})\Pr(\mathcal{H}_j|\mathbf{y}_{1:k-1}, \mathbf{u}_{1:k-1})}\end{aligned} \tag{13}$$

From eq. (10b) we have that the measurement is Gaussian distributed with mean $\hat{\mathbf{y}}_k$ and covariance $\mathbf{S}_k$ for a given series of measurements and control inputs, i.e. $p(\mathbf{y}_k|\mathbf{y}_{1:k-1}, \mathbf{u}_{1:k}) = \mathcal{N}(\mathbf{y}_k; \hat{\mathbf{y}}_k, \mathbf{S}_k)$. For a given hypothesis, and therefore also for a given measurement prediction, the analytical expression for the distribution of $\mathbf{y}_k$ is

$$\begin{aligned}\mathbf{p}(\mathbf{y}_k|\mathcal{H}_i, \mathbf{y}_{1:k-1}, \mathbf{u}_{1:k}) = \mathcal{N}(\mathbf{y}_k; \hat{\mathbf{y}}_{i,k}, \mathbf{S}_{i,k}) &= \frac{1}{\sqrt{(2\pi)^2|\mathbf{S}_{i,k}|}} e^{-\frac{(\mathbf{y}_k - \hat{\mathbf{y}}_{i,k})^\top \mathbf{S}_{i,k}^{-1}(\mathbf{y}_k - \hat{\mathbf{y}}_{i,k})}{2}} \\ &= \frac{1}{\sqrt{(2\pi)^2|\mathbf{S}_{i,k}|}} e^{-\frac{\boldsymbol{\nu}_{i,k}^\top \mathbf{S}_{i,k}^{-1}\boldsymbol{\nu}_{i,k}}{2}}\end{aligned} \tag{14}$$

Denoting the likelihoods of hypothesis i at time step k as $h_{i,k}$, and inserting the expression for the hypothesis conditional measurment distributions in eq. (14), the expression in eq. (13) becomes

$$h_{i,k} = \frac{\frac{1}{\sqrt{(2\pi)^2|\mathbf{S}_{i,k}|}} e^{-\frac{\boldsymbol{\nu}_{i,k}^\top \mathbf{S}_{i,k}^{-1} \boldsymbol{\nu}_{i,k}}{2}} \cdot h_{i,k-1}}{\sum_{j=1}^{3} \frac{1}{\sqrt{(2\pi)^2|\mathbf{S}_{j,k}|}} e^{-\frac{\boldsymbol{\nu}_{j,k}^\top \mathbf{S}_{j,k}^{-1} \boldsymbol{\nu}_{j,k}}{2}} \cdot h_{j,k-1}} \tag{15}$$

4.3 Kalman Filter and Steady-State Kalman Filter Comparison

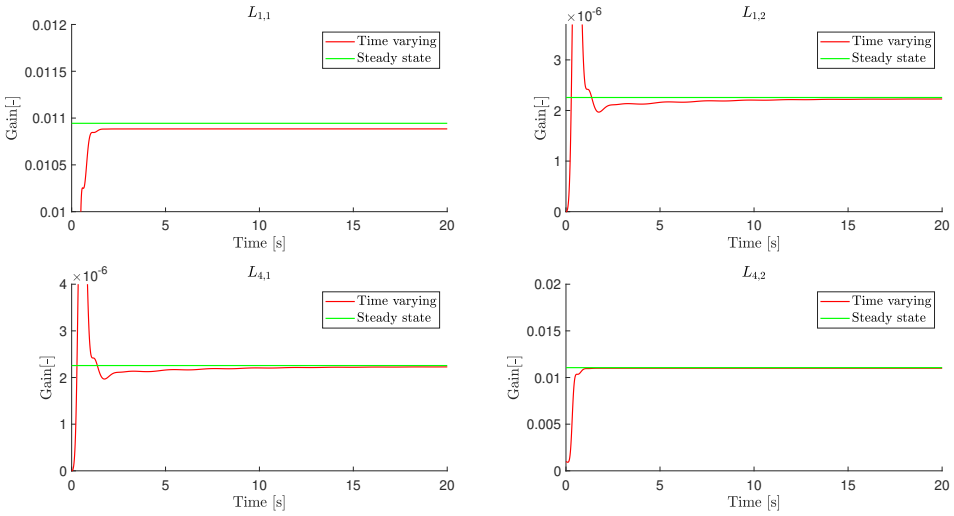

Figure 4: Samples of the Kalman gains from a time-varying - and steady-state Kalman filter.

In order to show convergence and justify the use of steady-state Kalman filters for the remainder of the exercise, a comparison of a time-varying and a steady-state Kalman filter for the same hypothesis is conducted. In fig. 4 one can see four samples of the Kalman gain from the two filters. As one can see, the gains of the time-varying Kalman filter converges quite quickly towards their steady-state equivalents. Specifically, one can say that the gains have converged after around 10 to 15 seconds. For the L_{11} and L_{42} gains there is evidence of some steady offsets. The reason for the offsets might be slight differences in the discretization methods for the two types of filters. Another possibility might also be that the offsets are not steady, but that the convergence rate for the two gains are so slow after 2 seconds, that they can be perceived as steady.

$$\mathbf{L_{KF}}(k = 300000) = \begin{bmatrix} 0.0109 & 0.0000 \\ 0.0001 & 0.0001 \\ 0.0001 & 0.0001 \\ 0.0000 & 0.0110 \\ 0.0596 & 0.0000 \\ 0.0031 & 0.0012 \\ 0.0012 & 0.0032 \\ 0.0000 & 0.0608 \\ 0.1859 & -0.0000 \\ -0.0000 & 0.1859 \end{bmatrix}, \quad \mathbf{L_{ssKF}} = \begin{bmatrix} 0.0109 & 0.0000 \\ 0.0001 & 0.0001 \\ 0.0001 & 0.0001 \\ 0.0000 & 0.0111 \\ 0.0597 & 0.0000 \\ 0.0032 & 0.0012 \\ 0.0012 & 0.0032 \\ 0.0000 & 0.0610 \\ 0.1858 & -0.0000 \\ -0.0000 & 0.1858 \end{bmatrix} \tag{16}$$

In eq. (16) one can see a comparison of the gain for the time-varying Kalman filter after 300000 time steps (300 seconds) and the steady-state Kalman filter gain. As one can see, the differences are minimal. Based on this and the above gain plots, it seems evident that the time-varying Kalman filter converges towards the steady-state Kalman filter. For this reason, for the following three cases only the results from the steady-state Kalman filters will be presented and discussed.

4.4 Case 1 - Results

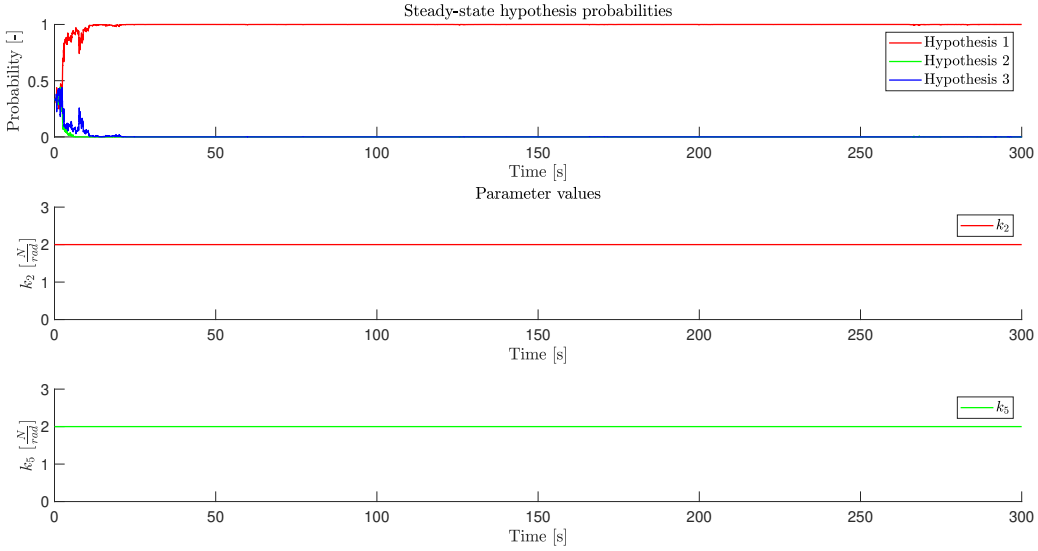

Figure 5: Simulation with $k_2 = k_5 = 2$.

4.5 Case 1 - Discussion

Case 1 tests the DHT for the plant with the same parameters as that of $\mathcal{H}_1$. One can see that the likelihood of $\mathcal{H}_1$ increases quite quickly and that it converges after approximately 10 seconds. The case validates that the correct hypotheses likelihoods is used and that the DHT it able to find the correct hypothesis when k_2 and k_5 are applied as the same values as that of one of the hypotheses. One can see that the DHT uses some time before the likelihood of the correct hypothesis converges to 1. This time delay is most is most likely the result of the DHT needing to get enough measurements to build confidence in a hypothesis before it can safely say that it is likely or not. However the results suggests that DHT can be a simple, yet valid technique for finding plausible model parameter values for real world applications, where the underlying plant model is unknown.

Despite the fact that the DHT deems the correct hypothesis the most likely one for constant inputs, the first case does not verify likelihood convergence when k_2 and k_5 are unequal to the parameter values of one of the hypotheses or dynamic. As the physical constants can vary over time as a result of operating conditions, such as temperature, it is also of interest to investigate how the DHT responds to varying values of k_2 and k_5.

4.6 Case 2 - Results

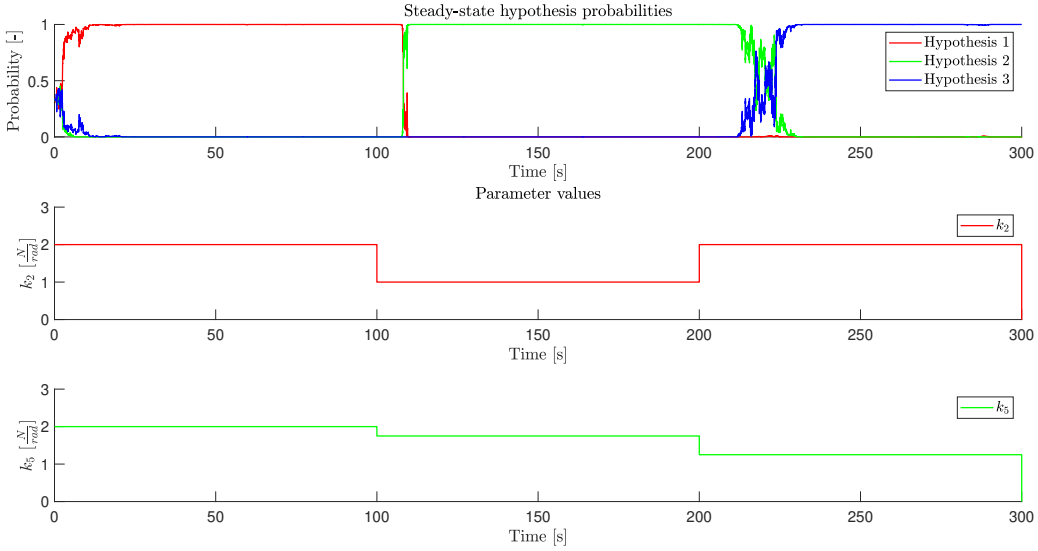

Figure 6: Simulation with steps between the different hypotheses.

4.7 Case 2 - Discussion

Case 2 tests the response of the DHT when the parameter values for the different hypotheses are applied in series through step-functions. The results in fig. 6 shows that the DHT is able to distinguish the correct hypothesis as the most likely one within their respective time intervals. Similarly to case 1 one can see that there is some time delay between the moment the parameters change to the DHT regards the correct hypothesis as the most likely one, as seen around 1, 100 and 200 seconds into the simulation. Again, this is most likely due to the DHT needing to receive a substantial number of measurements before it can consider a hypothesis to be more likely than the others. One can see that the likelihood transition from hypothesis one to two is much more distinct than the one from hypothesis two to three. This is evidence that dynamics of the plant are more distinguishable with the parameter values of hypothesis one and two, than with the parameters of hypothesis two and three.

4.8 Case 3 - Results

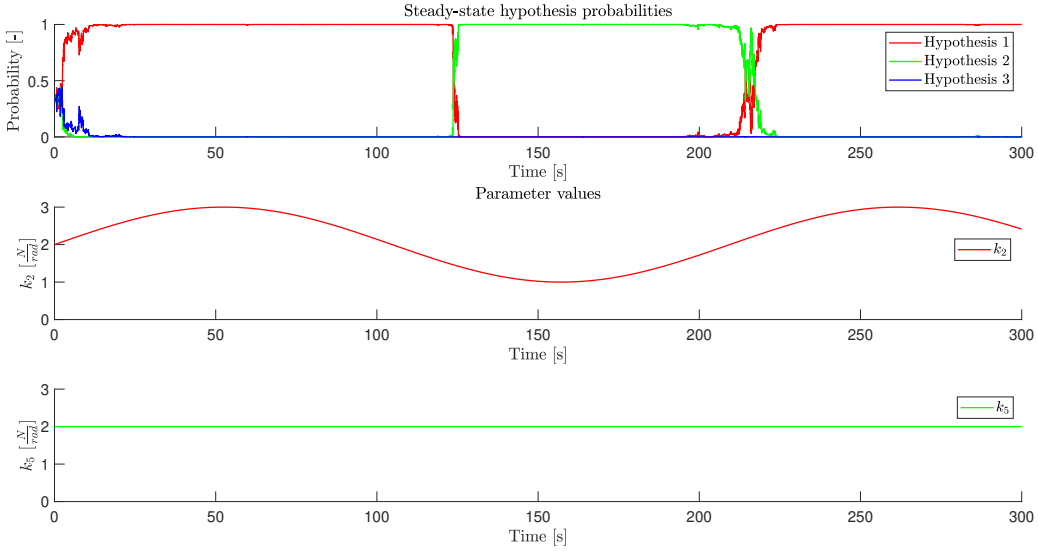

Figure 7: Simulation with oscillating k_2 and constant k_5.

4.9 Case 3 - Discussion

Case 3 tests the DHT under oscillating values for k_2 between 1 $[\frac{N}{rad}]$ and 3 $[\frac{N}{rad}]$, and a constant k_5 with value equal to 2 $[\frac{N}{rad}]$. Intuitively, a hypothesis was made that this would cause oscillations in the most likely hypothesis between $\mathcal{H}_1$ and $\mathcal{H}_3$, as the two parameter configuration extremes were closer to them. However as k_2 moves towards a value of 1 $[\frac{N}{rad}]$ the DHT finds $\mathcal{H}_2$ the most likely hypothesis. This suggests that the physical constant k_2 and k_5 have quite different effects on the dynamics of the plant. Additionally, one can see that the likelihood transitions are quite distinct, further backing up the hypothesis that the plant dynamics are quite similar under the parameter values of $\mathcal{H}_1$ and $\mathcal{H}_2$.

5 Conclusion

In this study a Kalman filter was implemented for a stochastic linear time-invariant model of a motor. The Kalman filter was then used to estimate the state of a linear plant with known parameters through noisy measurements and control inputs. The Kalman filter performance and consistency was then evaluated by analyzing the sequence of innovations and normalized innovations squared.

Then two filter assemblies were implemented, one with regular Kalman filters and one with steady-state Kalman filters, in order to perform dynamic hypothesis testing for a plant with some unknown parameters. Evidence that the regular Kalman filters converged to their steady-state equivalents were presented. Then dynamic hypothesis testing was performed with the steady-state Kalman filters for three different cases. The three cases covered scenarios where the plant parameters were static, quasi-static and dynamic. The likelihood response of the dynamic hypothesis testing were analyzed for the three cases.

1 Appendix

1.1 Model Matrices

$$\mathbf{A} = \begin{bmatrix} 0 & 0 & 0 & 0 & 1 & 0 & 0 & 0 & 0 & 0 \\ 0 & 0 & 0 & 0 & 0 & 1 & 0 & 0 & 0 & 0 \\ 0 & 0 & 0 & 0 & 0 & 0 & 1 & 0 & 0 & 0 \\ 0 & 0 & 0 & 0 & 0 & 0 & 0 & 1 & 0 & 0 \\ -\frac{k_1+k_2+k_3}{J_{L1}} & \frac{k_2}{J_{L1}} & \frac{k_3}{J_{L1}} & 0 & -\frac{b_1+b_2+b_3}{J_{L1}} & \frac{b_2}{J_{L1}} & \frac{b_3}{J_{L1}} & 0 & \frac{1}{J_{L1}} & 0 \\ \frac{k_2}{J_{M1}} & -\frac{k_2+k_4}{J_{M1}} & 0 & \frac{k_4}{J_{M1}} & \frac{b_2}{J_{M1}} & -\frac{b_2+b_4}{J_{M1}} & 0 & \frac{b_4}{J_{M1}} & 0 & 0 \\ \frac{k_3}{J_{M2}} & 0 & -\frac{k_3+k_5}{J_{M2}} & \frac{k_5}{J_{M2}} & \frac{b_3}{J_{M2}} & 0 & -\frac{b_3+b_5}{J_{M2}} & \frac{b_5}{J_{M2}} & 0 & 0 \\ 0 & \frac{k_4}{J_{L2}} & \frac{k_5}{J_{L2}} & -\frac{k_4+k_5}{J_{L2}} & 0 & \frac{b_4}{J_{L2}} & \frac{b_5}{J_{L2}} & -\frac{b_4+b_5}{J_{L2}} & 0 & \frac{1}{J_{L2}} \\ 0 & 0 & 0 & 0 & 0 & 0 & 0 & 0 & -.2 & 0 \\ 0 & 0 & 0 & 0 & 0 & 0 & 0 & 0 & 0 & -.2 \end{bmatrix} \tag{17}$$

$$\mathbf{B} = \begin{bmatrix} 0 & 0 \\ 0 & 0 \\ 0 & 0 \\ 0 & 0 \\ 0 & 0 \\ \frac{1}{J_{M1}} & 0 \\ 0 & \frac{1}{J_{M2}} \\ 0 & 0 \\ 0 & 0 \\ 0 & 0 \end{bmatrix} \tag{18}$$

$$\mathbf{G} = \begin{bmatrix} 0 & 0 \\ 0 & 0 \\ 0 & 0 \\ 0 & 0 \\ 0 & 0 \\ 0 & 0 \\ 0 & 0 \\ 0 & 0 \\ .2 & 0 \\ 0 & .2 \end{bmatrix} \tag{19}$$

$$\mathbf{C} = \begin{bmatrix} 1 & 0 & 0 & 0 & 0 & 0 & 0 & 0 & 0 & 0 \\ 0 & 0 & 0 & 1 & 0 & 0 & 0 & 0 & 0 & 0 \end{bmatrix} \tag{20}$$

2 References

References

Brekke, E., 2019. Fundamentals of sensor fusion: Target tracking, navigation and slam.

Brown, R.G., Hwang, P.Y.C., 2012. Introduction to Random Signals and Applied Kalman Filtering. Fourth ed., John Wiley Sons, Inc.